SLAC-PUB-14312

PRELIMINARY STUDY ON EMITTANCE GROWTH IN THE LHEC RECIRCULATING LINAC*

Yi-Peng Sun and Chris Adolphsen, SLAC, Menlo Park, USA
Frank Zimmermann, CERN, Geneva, Switzerland

Abstract

In this paper, we estimate the emittance growth in the LHeC recirculating Linac, the lattice design of which is presented in another paper of IPAC10 proceedings. The possible sources for emittance growth included here are: energy spread from RF acceleration in the SRF (superconducting RF) linac together with large chromatic effects from the lattice, and synchrotron radiation (SR) fluctuations in the recirculating arcs. 6-D multi-particle tracking is launched to calculate the emittance from the statistical point of view. The simulation results are also compared with a theoretical estimation.

INTRODUCTION

The accelerator chain of the LHeC Recirculating Linac consists of one linac equipped with SRF cavities, two arcs and one transfer line, the lattice design of which is presented in another paper of IPAC10 proceedings [1] [2].

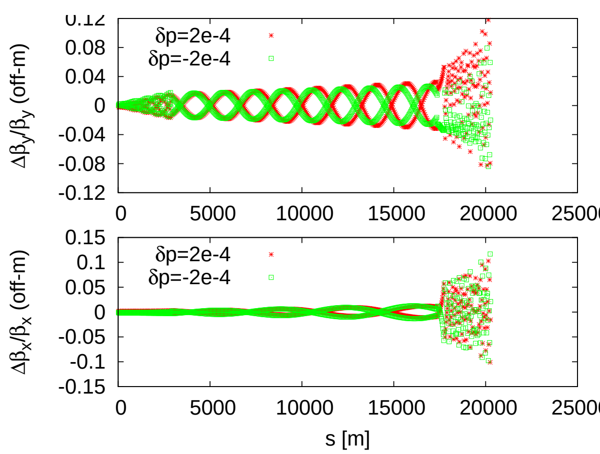

Figure 1: Off-momentum beta-beating in the LHeC Recirculating Linac, with two beam passes through the SRF linac, with $\delta p = \pm 2 \times 10^{-4}$. 1st pass in SRF linac: 0-3 km; 1st half arc: 3-9 km; straight transfer line: 9-12 km; 2nd half arc: 12-18 km; 2nd pass in SRF linac: 18-21 km.

The large beta functions in the second pass of the SRF linac, and in the transition regions between the arc and the linac, contribute to a large chromaticity which could thereafter introduce emittance growth (coupling between momentum and betatron motion). Further study is still ongoing to smooth the beta-function transitions, and if necessary to use arc sextupoles for the correction of the off-momentum beta beating. In Figure 1 the off-momentum beta-beating ($\delta p = \pm 2 \times 10^{-4}$) is plotted for the LHeC Recirculating Linac. The maximum beating is 12% in both horizontal and vertical planes. The peak of the beating occurs in the second pass of the SRF linac. Another source of emittance growth considered in this paper is the quantum phenomenon of the synchrotron radiation fluctuations, which is not an adiabatic process.

* Work supported by the European Community-Research Infrastructure Activity under the FP6 "Structuring the European Research Area" programme (CARE, contract number RII3-CT-2003-506395), and under the FP7 "Capacities Specific Programme" (EuCARD, under Grant Agreement no 227579). Work also supported by the DOE under Contract DE-AC02-76SF00515.

SIMULATION SETUP

MADX code

The MADX code [3] is an accelerator design and tracking code, which mainly considers single particle dynamics and is somehow constrained to a dedicated beam energy. Several new subroutines were added in the MADX thin-lens tracking module, to include the function of RF acceleration (adiabatic damping) in RF cavities, chromatic effects in the magnets (primarily energy dependent quadrupole strength), six dimensional macro-particle tracking (10,000 macro-particles), statistical treatment of the macro-particle's coordinates, emittance and bunch size calculation, as well as magnet power ripple and other error sources.

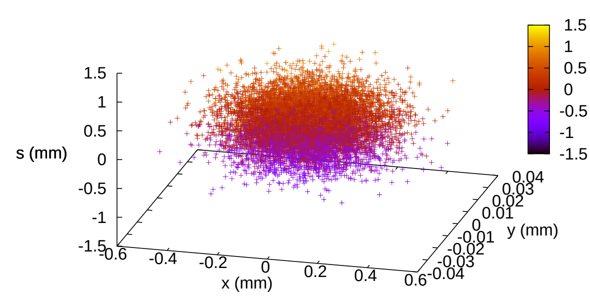

Figure 2: 6-D bunch distribution.

Generation of the bunch

A new subroutine 'trbunch' was added in the MADX thintrack module, to track a bunch of macro-particles (up to 10,000) at the same time, and to calculate the bunch emittance and beam size via a statistical treatment. 10,000 particles in a 6-D Gaussian distribution are generated inside MADX, using a FORTRAN code, for the design beam parameters such as the normalized emittance. The injection energy, TWISS parameters at the injection point, RMS bunch length and energy spread are also taken into account. A cut on the longitudinal distribution is performed at 3σ. Then the physical coordinates (x, x', y, y', ct, δp) of these 10,000 particles are tracked through the LHeC Recirculating Linac lattice. The tracking is done element by element. At specified places the emittance ϵ and bunch size σ are calculated by the following formulae and written to a file.

$$\sigma = \sqrt{\frac{1}{N}\sum_{i=1}^{N}(x_i - \bar{x})^2} \quad (1)$$

$$\epsilon = \sqrt{\overline{x^2}\cdot\overline{x'^2} - (\overline{xx'})^2} \quad (2)$$

where N denotes the number of macro-particles, and

$$\overline{x^2} = \frac{1}{N}\sum_{i=1}^{N} {x_i}^2, \overline{x'^2} = \frac{1}{N}\sum_{i=1}^{N} {x'_i}^2, \overline{xx'} = \frac{1}{N}\sum_{i=1}^{N} x_i {x'}_i. \quad (3)$$

In Figure 2 one sample bunch distribution consisting of 10,000 macro-particles is plotted in the $x - y - ct$ space.

SIMULATION RESULTS

Acceleration and radiation energy loss

The acceleration is achieved through the SRF cavities, the arrangement of which inside the linac cells is described in [1]. In Figure 3 (left) it is clearly seen how the electron beam is accelerated in two passes. The beam loses energy due to synchrotron radiation in the arc sections, which is demonstrated in the zoomed view of Figure 3 (right). For a final beam energy of 140 GeV, the beam energy is 70 GeV in the arcs and the energy loss is roughly 2% with a bending radius of 1500 m.

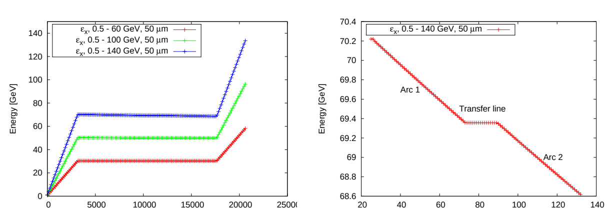

Figure 3: Left: energy versus longitudinal positions in the LHeC Recirculating Linac (two passes, final energy of 60 GeV, 100 GeV or 140 GeV); Right: energy loss in the two arc sections (final energy 140 GeV).

The RMS bunch length of the injected beam is chosen to be 300 μm, and the RMS energy spread $\sigma_e = 1 \times 10^{-4}$. The relative energy spread is plotted in Figure 4 along the lattice (two passes). It is determined by the bunch length, the RF frequency (700 MHz), and the instantaneous beam energy; and it basically scales inversely with $1/E$.

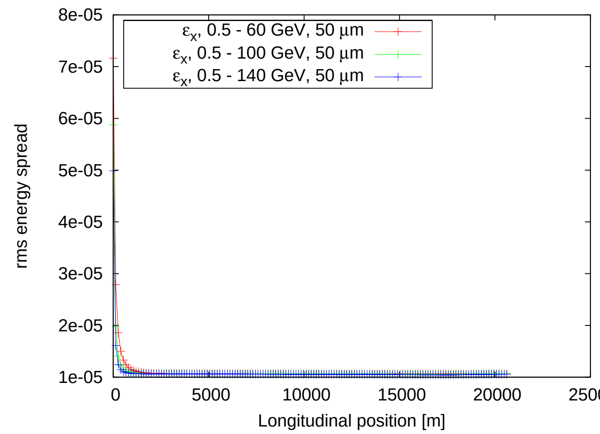

Figure 4: Relative energy spread.

Emittance growth only from chromaticity

As mentioned before, momentum dependent magnetic focusing can introduce emittance growth. The latter is investigated by simulations, as shown in Figure 5. The final emittance growth is less than 10%. There is a sharp increase in the transition region between the arc section and the second pass of the SRF linac, which is due to the huge beta function changes there. For larger beam energy, there is larger relative emittance growth where the β-peaks are higher and, accordingly, the chromaticity is also higher.

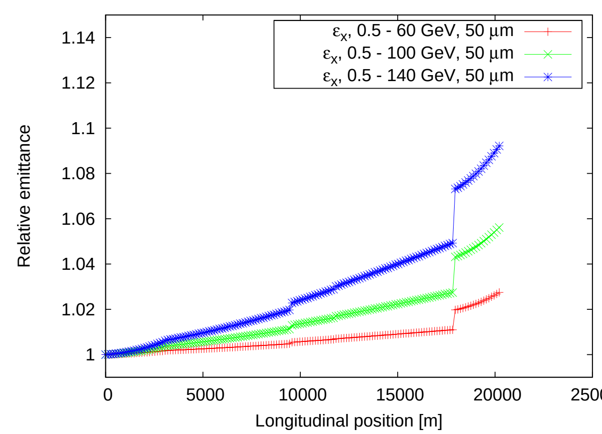

Figure 5: Relative emittance (horizontal plane) for three final beam energies (60 GeV, 100 GeV and 140 GeV), initial emittance is 50 μm.

At the same beam energy $E = 140$ GeV, the relative emittance growth is similar, for three cases with different initial emittance, as shown in Figure 6.

Emittance growth from chromaticity plus SR fluctuations

Synchrotron radiation is the electromagnetic radiation which is emitted from relativistic and accelerated charged particles. For particles in a bunch, this quantum process

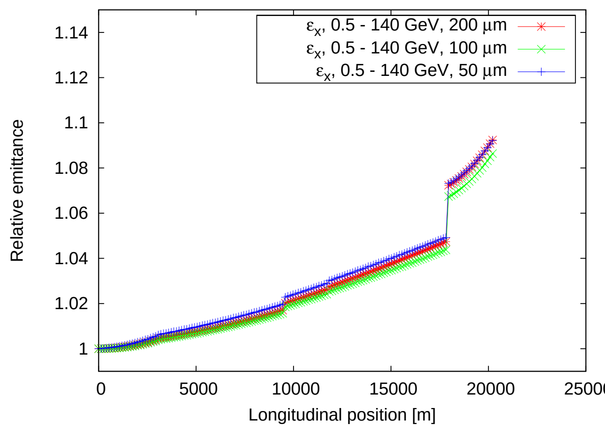

Figure 6: Relative emittance (horizontal plane), $E = 140$ GeV, initial emittance is 50 μm, 100 μm and 200 μm, respectively.

is random. That means when a charged particle passes through a dipole magnet and is accelerated orthogonally to its trajectory, it has a random probability of emitting a photon at any given time. Due to that reason, particles which have similar energy and coordinates may lose different amounts of energy at different times, and this difference in energy change will cause them to follow different trajectories and result in beam emittance growth [4].

For an electron beam with energy E and following a trajectory with bending radius ρ, the normalized emittance growth through the whole arc is [5]

$$\Delta\gamma\epsilon_x = 6.2 \times 10^{-5}\ \mathrm{GeV}^{-6}\mathrm{m}^2\ \frac{E^6}{\rho D^3} F \qquad (4)$$

where $\Delta\gamma\epsilon_x$ denotes the normalized emittance growth, D the number of dipole magnets which the beam passes through, and F a numerical factor determined by the lattice.

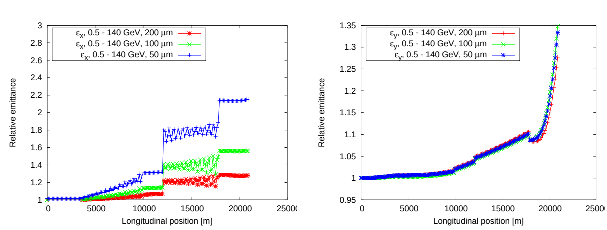

Figure 7: Relative emittance, $E = 140$ GeV, initial emittance is 50 μm, 100 μm and 200 μm, respectively. Left: horizontal plane; Right: vertical plane.

Using three different normalized initial emittances (50 μm, 100 μm and 200 μm) to generate the bunch distribution, and then track this bunch of particles through the LHeC recirculating linac (with quantum radiation in the arc), the relative emittance is calculated. The results are plotted in Figure 7. As there is no vertical dispersion, the relative emittance growth in the vertical plane is purely chromatic and independent of the initial emittance. In the horizontal plane, the absolute normalized emittance growth is similar for these three cases, about equal to an absolute increase of 50 μm. So the relative growth is largest for $\gamma\epsilon_x = 50$ μm, as shown in Figure 7 (left).

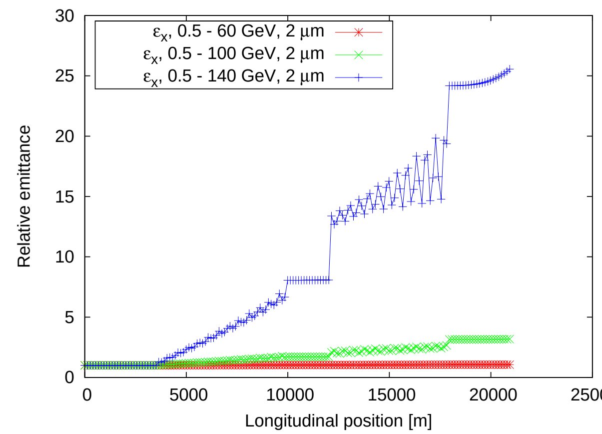

Figure 8: Relative emittance for three final beam energies (60 GeV, 100 GeV and 140 GeV), initial emittance is 2 μm.

As a final check, we choose the normalized emittance $\gamma\epsilon_x = 2$ μm from the European XFEL design [6], and repeat the simulation with synchrotron radiation effects. The emittance growth results are shown in Figure 8. For $E = 140$ GeV, the absolute normalized emittance growth is roughly 50 μm which is consistent with the estimate of Formula (4), and with the results of Fig. 7.

SUMMARY

Preliminary simulation studies show that the absolute normalized emittance growth is less than 50 μm from chromatic effects plus synchrotron radiation, with a final electron beam energy as 140 GeV. With an initial normalized emittance of 50 μm (which is almost preserved at 60 GeV and doubles to 100 μm at 140 GeV), the electron-beam physical emittance is about 4.3×10^{-10}m, which can provide efficient collisions with LHC protons ($\epsilon_x = 5 \times 10^{-10}$m) at the LHeC Interaction Point.

We acknowledge helpful discussions with Frank Schmidt of CERN.

REFERENCES

[1] Y.-P. Sun, THPD012, in IPAC10 proceedings.

[2] A. Eiders, Optics Development for the Recirculating Linac of a High-Energy Hadron-Lepton Collider (LHeC) at the LHC, NTNU Project Thesis (2009).

[3] MADX manual, http://mad.web.cern.ch/mad/.

[4] M. Sands, SLAC Report 121 (1970).

[5] C. Adolphsen et al., SLAC Report 474, Vol. 2, page 649 (1996); R. H. Helm, M. J. Lee, P.L. Morton, M. Sands, SLAC-PUB-1193 (1973).

[6] M. Altarelli et al., The Technical Design Report of the European XFEL, DESY (2007).